


# Comparative analysis of microstructure and quality of gas metal arc welded and shielded metal arc welded joints

R. Bendikienė\*, G. Janušas\*\*, D. Žižys\*\*\*

\*Kaunas University of Technology, Studentų 56, 51424 Kaunas, Lithuania, E-mail: regita.bendikiene@ktu.lt

\*\*Kaunas University of Technology, Studentų 56, 51424 Kaunas, Lithuania, E-mail: giedrius.janusas@ktu.lt

\*\*\*Kaunas University of Technology, Studentų 56, 51424 Kaunas, Lithuania, E-mail: kat0715@ktu.lt

 <http://dx.doi.org/10.5755/j01.mech.21.3.9861>

## 1. Introduction

Welding, the fusing of the surfaces of two work pieces to form one is a precise, reliable, cost-effective, and convenient method for joining metal alloys. No other technique used by manufacturers to join metals and alloys in such a big extent, because welding is a fast and economical process to compose joint of two different materials. Actually, many products such as building constructions, pipelines, automobiles, and others could not be made without the use of welding [1-3].

Every year, a lot of rejects appear due to poor techniques of welders, lack of control or choice of poor materials in order to save a fraction of expenses.

The welding processes found their own niche in metal production and manufacturing industry. Numerable welding techniques used in practise include submerged arc welding [4], tungsten inert gas welding [1, 5], metal inert gas welding [2], plasma arc welding [6] and etc.

In fusion welding processes, a metal alloy undergoes large local structural changes. The thermal expansion of the weld metal and nearby areas is restricted by the surrounding cold metal. This initiates the formation of residual plastic strains in the weld metal and the nearby area. These plastic strains are referred to as characteristic strains and are considered to be responsible for causing welding deformations and further defects of the weldment. Once the relation between the welding heat input and the characteristic strain distribution is established, the residual stress and deformation can be calculated by elastic analysis using characteristic strain as initial strain [5].

The main target of this study is to compare two of the most commonly used types of welding to make a joint and to evaluate quality and microstructure [7] of welds.

Gas metal arc welding (GMAW) is widespread for plastically deformed or closed parts of the automobile body and is frequently used where the part geometry restricts the application of resistance spot welding (RSW) or when the design requires supplementary joint strength and stiffness. The application of arc welding and flash butt welding processes for steel welding has also been reported [8]. The joined parts using GMAW typically undergoes a higher heat input and lower heating and cooling rates than other welding techniques in automotive applications. During GMAW welding, the microstructure is effected by metal arc heat different from that used for its production. Local heat input of the welding heat source that induces a large temperature gradient on the work piece changes the microstructure, and hence the mechanical properties.

GMAW is very useful due to its flexibility, possi-

bility to weld metals of different thickness, high production capability, and possibility of automatic implementation. As in many other types of welding, the weld geometry and molten pool thermal properties are controlled in order to increase the mechanical strength of weld connections and reduce the presence of weld defects and in general, increase the quality of weld [9].

Shielded metal arc welding (SMAW) can be performed on different materials of different thickness as well. This explains why repair welding has conventionally been carried out by manual SMAW operations [10]. The metal coalescence of SMAW is heated by an electric arc between the covered metallic electrode and the base metal. The electrode consumes itself during the SMAW process. Shielding is obtained from the decomposition of the electrode covering. Filler metal is obtained from the electrode. The arc is initiated by momentarily touching of the electrode to the base metal. The heat of the arc melts the surface of the base metal to form a molten pool at the end of the electrode.

The aim of this work is to quantify the microstructure in different parts of the GMAW and SMAW welded joints and to make a qualitative correlation between the microstructure, quality and the tensile strength of the welded joint.

## 2. Materials and experimental procedures

The material used in this research as base metal was non-alloy structural steel S235JR. It was chosen for the analysis and quality evaluation of welded joints using GMAW and SMAW technologies; steel characteristics are given in Table 1.

Table 1

Characteristics of steel S235JR

Steel grade	C % for nominal thickness of metal		
	≤ 16	>16 ≤40	> 40
S235JR*	≤ 0.17	≤ 0.17	≤ 0.20
Chemical composition, %			
Mn	P	S	CEV
1.40	0.035	0.035	0.012
0.35 – 0.40			
Characteristic yield strength $\sigma_y = 235$ MPa			
Characteristic ultimate strength $\sigma_u = 360$ MPa			
Countable yield strength $\sigma_{y,d} = 215$ MPa			
Countable ultimate strength $\sigma_{u,d} = 325$ MPa			
Nominal thickness of base metal – ≤ 16 mm			
* Steel grade according to LST EN 10027-1			

Presented steel grade is suitable for cold forming such as bending, folding, bordering, flanging, etc. It pos-

sesses good weldability with conventional welding processes. In most cases, pre- or post-heat treatment is not necessary when it comes to welding. Steel S235JR is applied for building components, containers, and storage tanks and for rolled profiles. With distinctly closer chemical composition values and mechanical properties, the steel grades of the S235–S355 series are used as material for wheels of passenger cars, Lorries and other vehicles.

Maximum carbon equivalent value:

$$CE = C + Mn/6 + (Cr + Mo + V)/5 + (Cu + Ni)/15 = 0.35.$$

Welding samples of the non-alloy structural steel (dimensions specified in Fig. 1) were machined according to Lithuanian standards. The welding was done in two passes. Six specimens were welded using SMAW method and six using GMAW technique. The welding scheme is shown in Fig. 2.

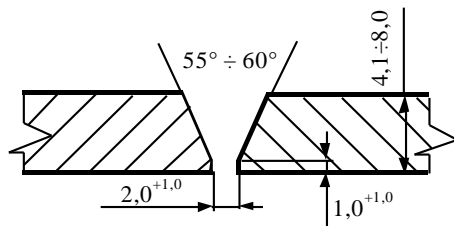


Fig. 1 Dimensions and allowable deviations of welding sample

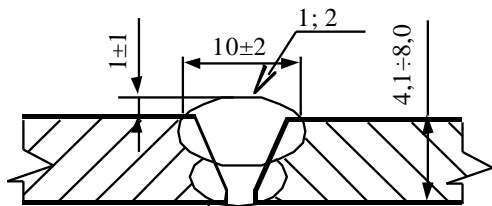


Fig. 2 The welding scheme

The composition of shielding gas used was: 82% argon, 18% CO<sub>2</sub> and < 0.03% NO. OK Autrod 12.50 coated non-copper filler metal was used as filler metal. The microstructural analysis of ground, polished and etched specimen was performed using optical microscopy. The test pieces for light optical microscopy (LOM) examination were prepared in longitudinal direction towards the welding seam in order to see all specific zones of the weld (heat affected zone). Also test pieces were polished up to fine diamond (~1 μm) finish and etched chemically for 10–30 sec. using solution: 2 volume parts of nitric acid, 98 volume parts of alcohol (nital reagent) and saturated solution of picric acid in alcohol (picral). Afterward, the screening of microstructures was done using a light microscope LMA 10 equipped with the YCH 15 camera, magnification of images 100<sup>x</sup>. To analyse the microstructure of the welded sample, the following areas were selected for microstructural analysis (Fig. 3).

It can be seen from the figures, that the welding was done in two passes. The distinctive areas from 1 to 5 show the microstructure inside the weld, while areas from 6 to 13 show the heat affected zone. There, the melting of base metal and filler metal was expected to be seen.

Areas from 15 to 18 show the base metal; it was expected to be intact and not affected by the heat in the welding seam. The highest temperature, as well as the biggest microstructure change, was expected in the welding

pool. The temperature drop was inversely proportional to the distance from the welding pool. The other important zone is HAZ. Micro structural changes may affect the mechanical properties of the weld (possible brittle martensite formation).

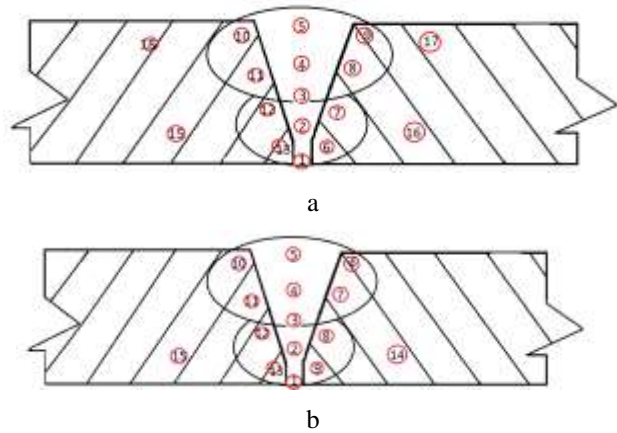


Fig. 3 Test areas for microstructure analysis of weld: a) GMAW, b) SMAW

Ferrite and ferrite with tertiary cementite was expected to form in the boundary zones. Three main zones were expected at HAZ: sub-critical, heated to less than 723°C, free of austenite, with some stress relief; inter-critical, partial austenite formation on heating which reverts to ferrite pearlite on cooling, and super-critical, complete transformation to austenite, grain refinement or the possibility of growth depending on maximum temperature.

### 3. Results

Two types of welding methods were used. For the evaluation of mechanical properties tensile specimens were made. The theoretical models characterise the intended model of grain structure formation due to melting and solidification of the weld. In this section, the obtained microstructure images will be compared to the intended theoretical models of HAZ and fusion zone micro-structure formation. The micro-structure investigation results will be compared to the tensile strength results [11] for a validation.

The grain size of test pieces was investigated, because it has a great effect on the ductility of material. It will be considered that the microstructure for all the test pieces that share similar welding types is comparatively the same and conclusions will be drawn on this basis.

#### 3.1. Analysis of GMAW test pieces microstructure

The analysis of the specimen was carried out with the 18 images taken in distinctive areas of HAZ of GMAW welded specimen.

The analysis was done according to the theoretical model of heat distribution and grain structure formation in relation to carbon percentage and temperature shown. The grain evaluation method, also known as Jeffries' Method was used for counting the average number of grains per known microstructure. This method helped to evaluate the effect of grain size on ductility of the test pieces.

Analysis of the obtained samples (areas from 1 to 5 shown in mapping of Fig. 3, a) indicated that the micro-

structure of given location mainly contained of ferrite (sample 1), and the structure was changing into pearlite + ferrite (sample 3 in Fig. 4) and then it revealed a considerable amount of pearlite in ferrite matrix (sample 5 as shown in Fig. 4).

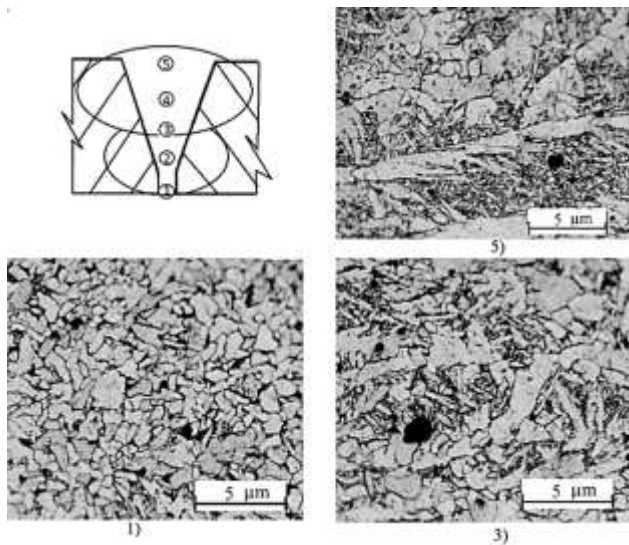


Fig. 4 Samples of GMAW microstructure (see Fig.3)

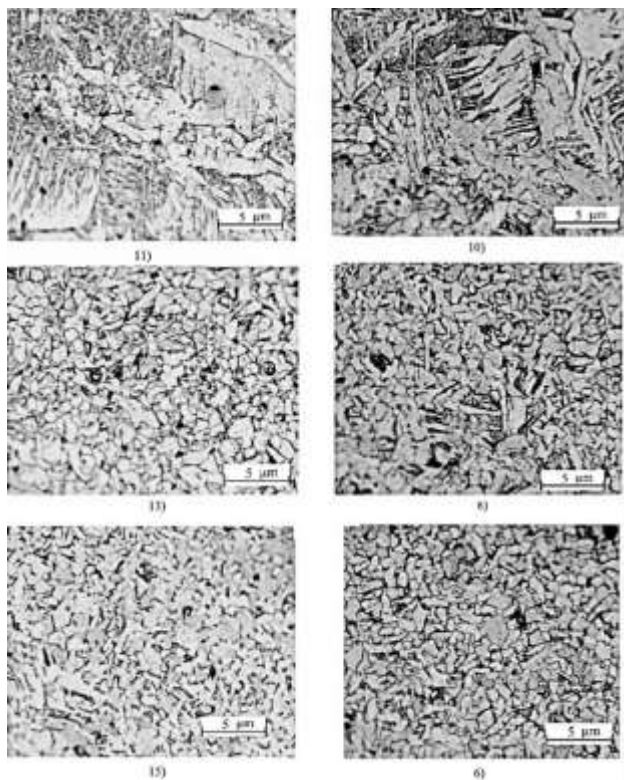


Fig. 5 Images of HAZ. Travelling down from the weld, the grain diameter gets finer, showing heat penetration. The structure composes mostly of ferrite

The investigation of areas further from welding bead confirmed the predictions that the structure should contain some pure ferrite with aligned carbides and pearlite + ferrite structures. The ferrite grains in the outer regions of the welding seam gets coarser, indicating the decreased ductility of the welding seam. The finer grains are characterised as having better mechanical properties than the metal of the same chemical composition though having more coarse grains: better tensile properties, higher yield

points and strength, fatigue resistance. The grain diameter varies from  $0.5 \mu\text{m}$  to  $4 \mu\text{m}$ , which mostly depends on temperatures reached and on the cooling rate.

The higher temperature, the coarser ferrite grains – the lower material ductility. Fig. 5 shows other distinctive areas of the welding seam and its microstructure. Judging on grain diameters and no presence of transformation products, the conclusion may be drawn that the specimens were not overheated and the cooling rate was enough, thus preserving material's ductility and strengthening the welding seam.

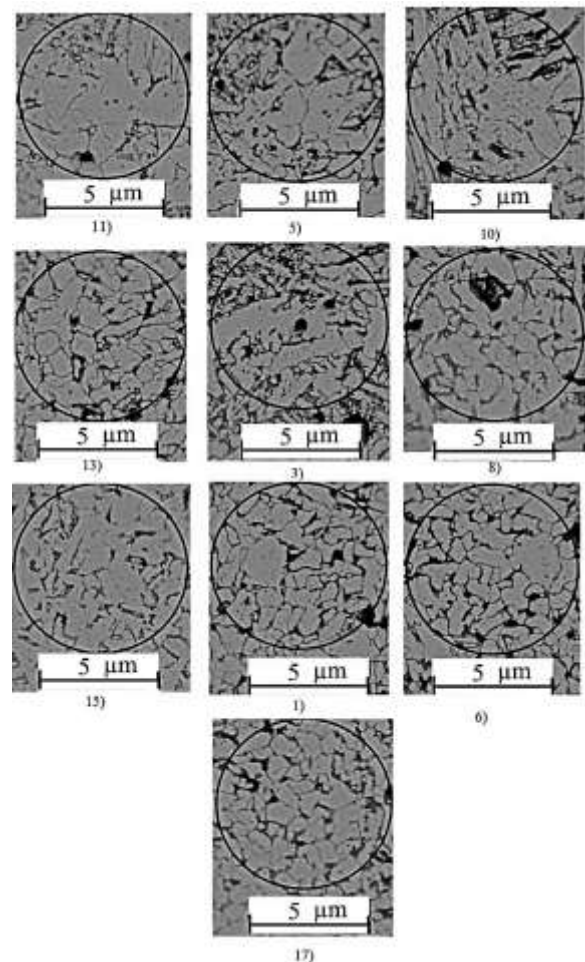


Fig. 6 Areas of test pieces showing different sizes of grains

The comparison of the grain size of GMAW welded specimens was done to find out how the grain size changes along the weld seam. The visual results, shown in Fig. 6, indicate that the grain sizes in the welding seam are quite coarse but change slightly depends on the location. The coarsest structure was found at the bottom of the weld (Fig. 3, a). The finest grains were found outside the welding seam (No. 17) and furthest from the welding surface with ASTM grain size number around 1. ASTM grain size number in the upper layers of HAZ is 0 and negative.

The comparison was done by inscribing a circle of a known area,  $A = 314 \text{ cm}^2$  on an image of  $100\times$  magnification. The number of grains completely falling into the area was counted, and then the number of grains partially falling into the area was counted and divided by 2. Both results are summed up and divided by the area of the circle. The results are the number of the grains per  $1 \text{ cm}^2$  at  $100\times$ .

3.2. Analysis of SWAW test pieces microstructure

The SMAW welded test pieces were found to be quite different from the GMAW ones.

Fig. 7 indicates that the central part of the weld has no fine ferrite; it remains similar through the whole welding seam and has assumed a needle-shaped form with coarse structure.

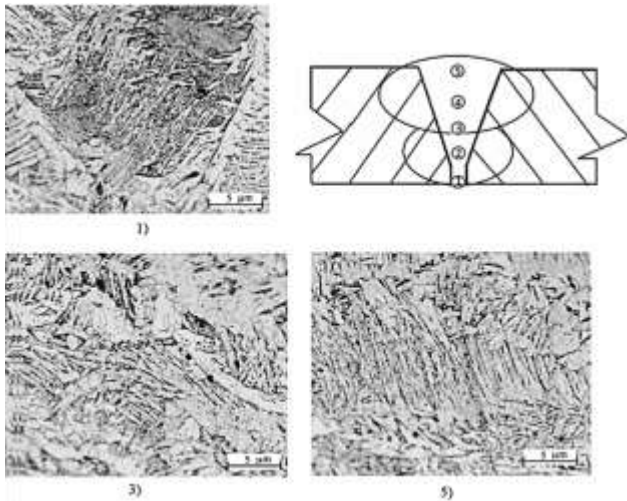


Fig. 7 SMAW test piece. Coarse, needle-shaped ferrite structure is seen through-out the whole section

This clearly indicates that the structure has been overheated and probably slightly hardened since the welding procedure took place in room temperature and this can have contributed towards poor weld condition and appearance of inner stresses. The mapping of the SMAW microstructure investigation specimen is seen in Fig. 3, b.

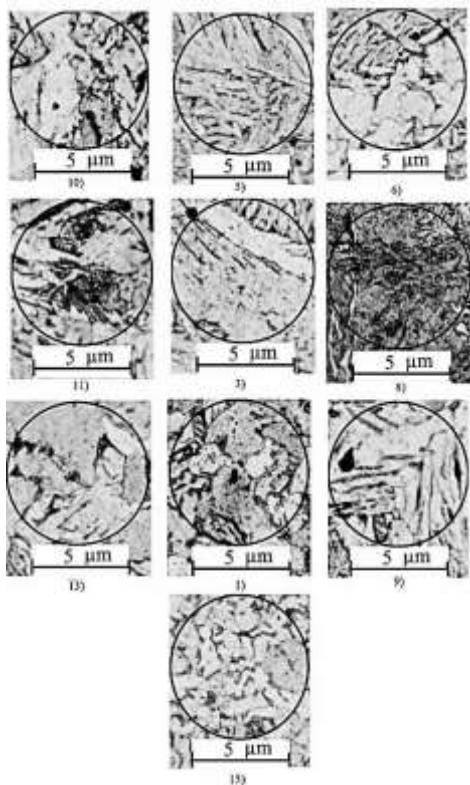


Fig. 8 Microstructure of joint between base metal and weld

Investigation of further locations of HAZ revealed that it is very similar to the central part of the welding seam. The microstructure images of test pieces' are seen in Fig. 8.

The dendrite and needle-shaped ferrite structure with coarse grains is seen everywhere. These features clearly indicate the overheating of the whole welding seam and possible hardening.

The comparison of SMAW welded test pieces' grain size was done to find out how the grain size changes along the weld seam. The visual results, shown in Fig. 9, indicate that the grain sizes in the welding seam are extremely coarse, differing significantly from the grain size out of weld. The exact results of grains per 1 cm<sup>2</sup> at 100<sup>x</sup> are given in Table 2.

Table 2  
Comparison of SMAW and GMAW welded test pieces grain size per cm<sup>2</sup> at 100<sup>x</sup>

	Left joint of base metal and weld		Center of welding seam		Right joint of base metal and weld	
	SMAW	GMAW	SMAW	GMAW	SMAW	GMAW
Grains in cm <sup>2</sup> at 100 <sup>x</sup>	0.02	0.04	0.04	0.06	0.03	0.03
	0.02	0.15	0.01	0.06	0.01	0.11
	0.02	0.11	0.01	0.14	0.02	0.15
Average grain in cm <sup>2</sup> at 100 <sup>x</sup>	0.02	0.10	0.02	0.09	0.02	0.10

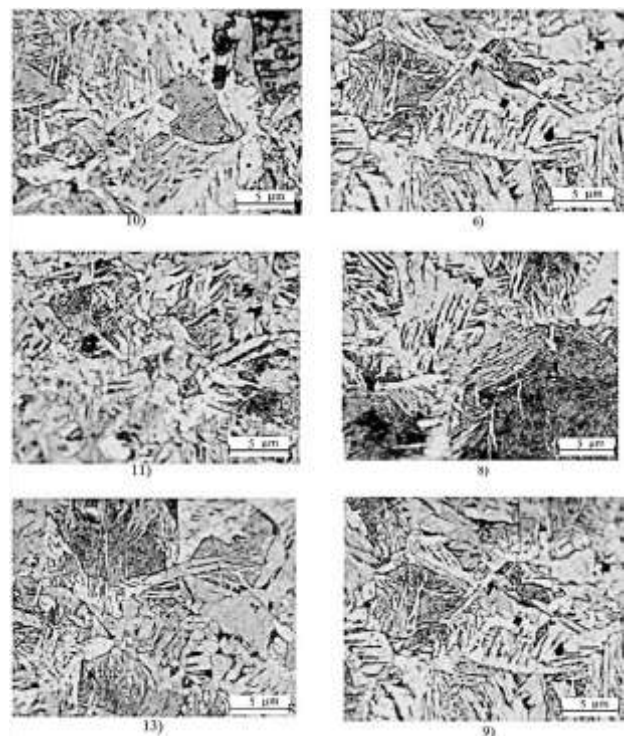


Fig. 9 Areas of the test piece showing different grains. The finest grains were found outside weld

3.3. Comparison of the results of microstructure investigation with the results of tensile strength test

Test results of the tensile strength performed in the work [11] and microstructure results partially coincide. The microstructure investigation of GMAW specimens

parallel to the results of tensile strength test; microstructure of GMAW specimen does not show any significant anomalies or faults done due to overheating of the welding seam or other characteristics of HAZ. On the other hand, the microstructure of SMAW specimens' show clear signs of overheating and signs of hardening that may have caused inner stresses of the structure and weakening of the welding seam. The coarse grain structure also confirms the conclusion of overheating, and the dendrite, needle-shaped ferrite structure speaks of partial hardening due to cold temperatures of the surroundings. Comparison of grain sizes of SMAW and GMAW specimens shown in Table 2.

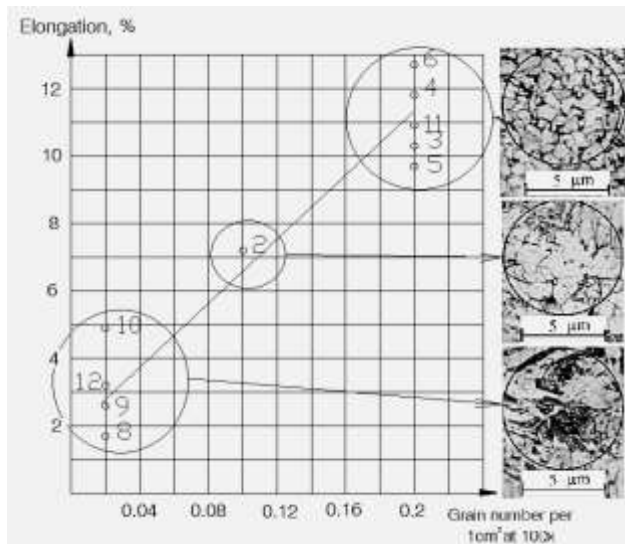


Fig. 10 Test pieces from 2 to 12 (GMAW specimens 2-6, SMAW specimens 8-12) compared according to elongation dependence from grain size

The comparison clearly shows that the microstructure of GMAW specimen weld seam contains 4 to 5 times more grains per  $\text{cm}^2$  than SMAW test pieces.

The one problem with the GMAW is that the weld

surface contains significantly coarser structure than the rest of GMAW weld. This may also indicate effect of cold air or local overheating of material.

The table and diagram (Fig. 10) were presented for the comparison of GMAW and SMAW test pieces according to location of failure, number of grains per  $\text{cm}^2$  at  $100\times$  and comparative elongation of specimens. This was done to demonstrate how specimens' ductility depends on the grain size.

Comparing results of microstructure investigation with results of tensile strength test, given in the Table 3 [11], correlation between both is clearly seen.

The coarse structure of SMAW test pieces welding seam resulted in loss of ductility and mechanical properties and thus in weakening of the welding seam as a whole. Most of SMAW test pieces have failed tensile strength test due to weakness of welding seam, thus failing demonstrates mechanical properties of base metal. The weakness of welding seam in SMAW test pieces was caused by two factors: macro structural faults of the welding seam (such as undercutting, lack of fusion, insufficient penetration, etc.) and micro structural faults, such as overheating or wrong temperature treatment chosen.

Failure of SMAW specimen was more of a rule than an exception in this particular analysed case.

GMAW specimens have sustained their strength and ductility, passing the test with one exception. Fig. 10 clearly indicates that GMAW test pieces are spread in the upper zone of the diagram, sustaining ductility and finer grain structure. The welding seam withstood the test; the fractures took place in the base metal instead of welding seams thus the standard indicates that the welding seam is required to hold 90% of maximum stress required for base metal. Micro structural investigation confirmed the results. No significant overheating was detected, thus indicating good quality of the welding seam. Failure of a GMAW specimen was more of an exception than a rule in this particular case.

Table 3

Comparison of SMAW and GMAW welded test pieces [11]

No.	Location of fracture	Min. allowed $\sigma_y$	Min. allowed $\sigma_u$	Actual $\sigma_y$	Actual $\sigma_u$	Status	Extent $\delta$ , %	Comparative contraction of cross-section $\psi$ , %	Faults*
2	Weld seam	213	324	143.9	395.7	Failed	7.2	16.2	4;
3	Base metal	235	360	243.0	427.0	Passed	10.3	43.6	0;
4	Base metal	235	360	275.5	420.1	Passed	11.8	48.5	0;
5	Base metal	235	360	243.0	427.0	Passed	9.7	44.9	0;
6	Base metal	235	360	238.8	432.0	Passed	12.7	59.5	0;
8	Weld seam	213	324	190.5	213.5	Failed	1.7	23.1	1; 2; 3; 4;
9	Weld seam	213	324	155.4	258.4	Failed	2.6	35.1	1; 5; 3;
10	Weld seam	213	324	162.0	260.3	Failed	4.9	45.2	1; 3; 4;
11	Base metal	235	360	236.8	432.0	Passed	10.9	51.4	1;
12	Weld seam	213	324	141.7	181.8	Failed	3.2	29.6	1; 4; 5;

#### 4. Conclusions

1. The grain size in GMAW test pieces varies from  $0.5 \mu\text{m}$  to  $4 \mu\text{m}$ , which is mostly dependent on temperatures reached and the cooling rate. The higher the temperature – the coarser the ferrite grains, on other hand the coarser the grains – the lower the material ductility. Finer grains are characterised as having better mechanical prop-

erties. The GMAW specimens were not overheated during welding, therefore giving it a strengthening effect.

2. The grains in SMAW welding seam are extremely coarse, differing significantly from the grain size out of welding seam. The microstructures of SMAW test pieces' show the clear signs of overheating and signs of annealing that cause inner stresses of the structure and weakening of the welding seam.

3. The comparison clearly shows that the microstructure of GMAW test piece weld seam contains 4 to 5 times more grains per  $\text{cm}^2$  than SMAW test pieces.

4. The coarse structure of SMAW test pieces welding seam resulted in the loss of both ductility and mechanical properties thus in weakening of the welding seam as a whole.

## References

1. **Hussain, A.K.; Lateef, A.; Javed, M.; Pramesh, T.** 2010. Influence of welding speed on tensile strength of welded joint in TIG welding process, *International Journal of Applied Engineering Research* 1(3): 518-527.
2. **Abbasi, K.; Alam, S.; Khan, M.I.** 2011. An experimental study on the effect of increased pressure on MIG welding arc, *International Journal of Applied Engineering Research* 2(1): 22-27.
3. **Leisis, V.; Zeleniakienė, D.; Griskevicius, P.; Jutas, A.; Ziliukas, A.; Meslinas, N.** 2008. Strength and stability assessment of underground composite tanks, *Proceedings of 13th International Conference Mechanics 2008*, 308-313.
4. **Murugan, N.; Gunaraj, V.** 2005. Prediction and control of weld bead geometry and shape relationships in submerged arc welding of pipes, *Journal of Materials Processing Technology* 168(3): 478-487. <http://dx.doi.org/10.1016/j.jmatprotec.2005.03.001>.
5. **Biswas, P.; Mandal, N.R.; Vasu, P.; Padasalag, S.B.** 2011. A study on port plug distortion caused by narrow gap combined GTAW & SMAW and electron beam welding, *Fusion Engineering and Design* 86(1): 99-105. <http://dx.doi.org/10.1016/j.fusengdes.2010.08.040>.
6. **Wang, Y.; Chen, Q.** 2002. On-line quality monitoring in plasma-arc welding, *Journal of Materials Processing Technology* 120(1-3): 270-274. [http://dx.doi.org/10.1016/S0924-0136\(01\)01190-6](http://dx.doi.org/10.1016/S0924-0136(01)01190-6).
7. **Ramazani, A.; Mukherjee, K.; Abdurakhmanov, A.; Prah, U.; Schleser, M.; Reigen, U.; Bleck, W.** 2014. Micro-macro-characterisation and modelling of mechanical properties of gas metal arc welded (GMAW) DP600 steel, *Materials Science and Engineering* 589: 1-14. <http://dx.doi.org/10.1016/j.msea.2013.09.056>.
8. **Hsu, C.; Soltis, P.; Barton, D.; Occhialini, C.** 2004. Weldability of dual-phase steel with arc welding Processes, *Sheet Metal Conference, XI Sterling Heights MI*: 1-11.
9. **Anzehae, M.N.; Haeri, M.** 2012. A new method to control heat and mass transfer to work piece in a GMAW process, *Journal of Process Control* 22(6): 1087-1102. <http://dx.doi.org/10.1016/j.jprocont.2012.04.004>.
10. **Tung, P.Ch.; Wu, M.Ch.; Hwang, Y.R.** 2004. An image-guided mobile robotic welding system for SMAW repair processes, *International Journal of Machine Tools and Manufacture* 44(11): 1223-1233. <http://dx.doi.org/10.1016/j.ijmachtools.2004.03.006>.
11. **Janušas, G.; Jutas, A.; Palevičius, A.; Žižys, D.; Barila, A.** 2011. Static and vibrational analysis of the GMAW and SMAW joints quality, *Journal of Vibroengineering* 14(3): 1220-1227.

R. Bendikienė, G. Janušas, D. Žižys

## COMPARATIVE ANALYSIS OF MICROSTRUCTURE AND QUALITY OF GAS METAL ARC WELDED AND SHIELDED METAL ARC WELDED JOINTS

### Summary

In this work a comparative study of two metal arc welding methods Gas Metal Arc Welding (GMAW or MIG) and Shielded Metal Arc Welding (SMAW) were performed as well as quality and microstructure of welds were compared. The first one is the welding type with consumable electrode and gas shielding, and the second one is the welding method with consumable, flux coated electrode especially used for repairing. To ensure the satisfactory performance of a welded structure, the quality of the welds was determined by adequate testing procedures. The tests were performed on specimens manufactured according to Lithuanian Standard Board requirements, specifically LST EN 895:1998. Test pieces made of structural steel S235JR (LST EN 10027-1) were subjected to welding. Obtained microstructures revealed differences between two welding methods used for experiments, while the evaluation of grain size confirmed the former results of tensile strength tests.

**Keywords:** grain size, GMAW, materials testing, microstructure, SMAW, welding

Received February 17, 2015

Accepted April 02, 2015